In every local Lorentz frame this will be a sum of products of curvature components, and it will have the same value $48M^2/r^6$. Thus, in every local Lorentz frame, including the traveler's, ***Riemann*** will have one or more infinite components as $r \longrightarrow 0$; i.e., tidal forces will become infinite.

At $r = 0$ the curvature is infinite

EXERCISE

Exercise 31.1. TIDAL FORCES ON INFALLING EXPLORER

(a) Carry out the details of the derivation of the Riemann tensor components (31.6).

(b) Calculate, roughly, the critical mass M_{crit} such that, if $M > M_{\text{crit}}$ the explorer's body (a human body made of normal flesh and bones) can withstand the tidal forces at $r = 2M$, but if $M < M_{\text{crit}}$ his body is mutilated by them. [Answer: $M_{\text{crit}} \sim 1000M_\odot$. Evidently, if $M \sim M_\odot$ the physicist should transform himself into an ant before taking the plunge! For details see §32.6.]

---

§31.3. BEHAVIOR OF SCHWARZSCHILD COORDINATES AT $r = 2M$

Nature of the coordinate pathology at $r = 2M$:

Since the spacetime geometry is well behaved at the gravitational radius, the singular behavior there of the Schwarzschild metric components, $g_{tt} = -(1 - 2M/r)$ and $g_{rr} = (1 - 2M/r)^{-1}$, must be due to a pathology there of the Schwarzschild coordinates t, r, θ, ϕ. Somehow one must find a way to get rid of that pathology—i.e., one must construct a new coordinate system from which the pathology is absent. Before doing this, it is helpful to understand better the precise nature of the pathology.

(1) t and r reverse roles as timelike and spacelike coordinates

The most obvious pathology at $r = 2M$ is the reversal there of the roles of t and r as timelike and spacelike coordinates. In the region $r > 2M$, the t direction, $\partial/\partial t$, is timelike ($g_{tt} < 0$) and the r direction, $\partial/\partial r$, is spacelike ($g_{rr} > 0$); but in the region $r < 2M$, $\partial/\partial t$ is spacelike ($g_{tt} > 0$) and $\partial/\partial r$ is timelike ($g_{rr} < 0$).

What does it mean for r to "change in character from a spacelike coordinate to a timelike one"? The explorer in his jet-powered spaceship prior to arrival at $r = 2M$ always has the option to turn on his jets and change his motion from decreasing r (infall) to increasing r (escape). Quite the contrary is the situation when he has once allowed himself to fall inside $r = 2M$. Then the further decrease of r represents the passage of time. No command that the traveler can give to his jet engine will turn back time. That unseen power of the world which drags everyone forward willy-nilly from age twenty to forty and from forty to eighty also drags the rocket in from time coordinate $r = 2M$ to the later value of the time coordinate $r = 0$. No human act of will, no engine, no rocket, no force (see exercise 31.3) can make time stand still. As surely as cells die, as surely as the traveler's watch ticks away "the unforgiving minutes," with equal certainty, and with never one halt along the way, r drops from $2M$ to 0.

At $r = 2M$, where r and t exchange roles as space and time coordinates, g_{tt} vanishes while g_{rr} is infinite. The vanishing of g_{tt} suggests that *the surface* $r = 2M$, *which*

(2) the region $r = 2M$, $-\infty < t < +\infty$ is two-dimensional rather than three

appears to be three-dimensional in the Schwarzschild coordinate system $(-\infty < t < +\infty,\ 0 < \theta < \pi,\ 0 < \phi < 2\pi)$ *has zero volume and thus is actually only two-dimensional, or else is null;* thus,

$$\int_{r=2M} |g_{tt}g_{\theta\theta}g_{\phi\phi}|^{1/2}\, dt\, d\theta\, d\phi = 0;$$
$$\int_{(r=2M,t=\text{const})} |g_{\theta\theta}g_{\phi\phi}|^{1/2}\, d\theta\, d\phi = 4\pi(2M)^2. \tag{31.8}$$

The divergence of g_{rr} at $r = 2M$ does *not* mean that $r = 2M$ is infinitely far from all other regions of spacetime. On the contrary, the proper distance from $r = 2M$ to a point with arbitrary r is

$$\int_{2M}^{r} |g_{rr}|^{1/2}\, dr = \begin{cases} [r(r-2M)]^{1/2} + 2M \ln|(r/2M-1)^{1/2} + (r/2M)^{1/2}| \\ \qquad\qquad \text{when } r > 2M, \\ -2M\cot^{-1}[r^{1/2}/(2M-r)^{1/2}] - [r(2M-r)]^{1/2} \\ \qquad\qquad \text{when } r < 2M, \end{cases} \tag{31.9}$$

which is finite for all $0 < r < \infty$.

Just how the region $r < 2M$ is physically connected to the region $r > 2M$ can be discovered by examining the radial geodesics of the Schwarzschild metric. Focus attention, for concreteness, on the trajectory of a test particle that gets ejected from the singularity at $r = 0$, flies radially outward through $r = 2M$, reaches a maximum radius $r_{\max}$ ("top of orbit") at proper time $\tau = 0$ and coordinate time $t = 0$, and then falls back down through $r = 2M$ to $r = 0$. The solution of the geodesic equation for such an orbit was derived in §25.5 and described in Figure 25.3. It has the "cycloid form" (with the parameter η running from $-\pi$ to $+\pi$),

$$r = \frac{1}{2} r_{\max}(1 + \cos\eta), \tag{31.10a}$$

$$\tau = (r_{\max}{}^3/8M)^{1/2}(\eta + \sin\eta), \tag{31.10b}$$

$$t = 2M \ln\left|\frac{(r_{\max}/2M-1)^{1/2} + \tan(\eta/2)}{(r_{\max}/2M-1)^{1/2} - \tan(\eta/2)}\right| + 2M\left(\frac{r_{\max}}{2M} - 1\right)^{1/2}\left[\eta + \left(\frac{r_{\max}}{4M}\right)(\eta + \sin\eta)\right]. \tag{31.10c}$$

Figure 31.1 plots this orbit in the r, t-coordinate plane (curve F-F'-F''), along with several other types of radial geodesics.

(3) radial geodesics reveal that the regions $r = 2M$, $t = \pm\infty$ are "finite" parts of spacetime

Every radial geodesic except a "set of geodesics of measure zero" crosses the gravitational radius at $t = +\infty$ (or at $t = -\infty$, or both), according to Figure 31.1 and the calculations behind that figure (exercises for the student! See Chapter 25). One therefore suspects that all the physics at $r = 2M$ is consigned to $t = \pm\infty$ by reason of some unhappiness in the choice of the Schwarzschild coordinates. A better coordinate system, one begins to believe, will take these two "points at infinity" and

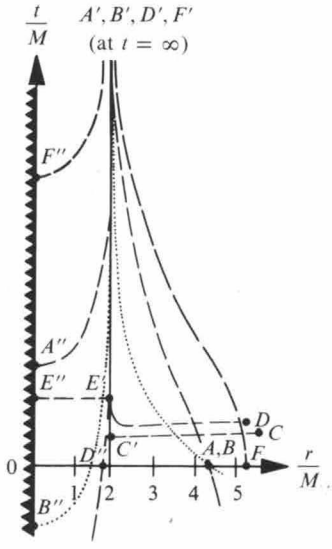

Figure 31.1.

Typical radial geodesics of the Schwarzschild geometry, as charted in Schwarzschild coordinates (schematic). $FF'F''$ [see equations (31.10)] is the timelike geodesic of a test particle that starts at rest at $r = 5.2M$ and falls straight in, arriving in a finite proper time at the singularity $r = 0$ (zig-zag marking). The unhappiness of the Schwarzschild coordinate system shows in two ways: (1) in the fact that t goes to ∞ partway through the motion; and (2) in the fact that t thereafter decreases as τ (not shown) continues to increase. The course of the same trajectory prior to $t = 0$ may be constructed by reflecting the diagram in the horizontal axis ("time inversion"). The time-reversed image of F'' marks the ejection of the test particle from the singularity. $AA'A''$ is a timelike geodesic which comes in from $r = +\infty$. $BB'B''$ is the null geodesic travelled by a photon that falls straight in (no summit; never at rest!). $DD'D''$ is a spacelike radial geodesic. So is CC', but $E'E''$ is timelike. Neither of the latter two ever succeed in crossing $r = 2M$. (Unanswered questions about these geodesics will answer themselves in Figure 31.4, where the same world lines are charted in a "Kruskal-Szekeres diagram").

Described mathematically via equation (31.10), the geodesic $F''_{\text{inverse}}\, F'_{\text{inverse}}\, FF'F''$ starts with ejection at

$$r = 0 \text{ at } t = -2\pi M\left(\frac{r_{\max}}{2M} - 1\right)^{1/2}\left(\frac{r_{\max}}{4M} + 1\right), \quad \tau = -\frac{\pi}{2}\left(\frac{r_{\max}^3}{2M}\right)^{1/2};$$

it flies outward with increasing proper time τ, but decreasing coordinate time, t, until it reaches the gravitational radius

$$r = 2M \text{ at } t = -\infty, \quad \tau = -\left(\frac{r_{\max}^3}{8M}\right)^{1/2}\cos^{-1}\left(\frac{4M}{r_{\max}} - 1\right) - r_{\max}\left(1 - \frac{2M}{r_{\max}}\right)^{1/2};$$

it then continues to fly on outward, but with coordinate time now increasing from $t = -\infty$, until it reaches its maximum radius

$$r = r_{\max} \text{ at } t = 0, \quad \tau = 0 \text{ (event } F \text{ in diagram);}$$

it then falls inward, with t continuing to increase, until it crosses the gravitational radius again

$$r = 2M \text{ at } t = +\infty, \quad \tau = +\left(\frac{r_{\max}^3}{8M}\right)^{1/2}\cos^{-1}\left(\frac{4M}{r_{\max}} - 1\right) + r_{\max}\left(1 - \frac{2M}{r_{\max}}\right)^{1/2}$$
$$\text{(event } F' \text{ in diagram);}$$

and it finally falls on in with decreasing t (but, of course, still increasing τ) to

$$r = 0 \text{ at } t = +2\pi M\left(\frac{r_{\max}}{2M} - 1\right)^{1/2}\left(\frac{r_{\max}}{4M} + 1\right), \quad \tau = +\frac{\pi}{2}\left(\frac{r_{\max}^3}{2M}\right)^{1/2}$$
$$\text{(event } F'' \text{ in diagram).}$$

variables u and v in which the line element has the form

$$ds^2 = f^2(u,v)(dv^2 - du^2) - r^2(d\theta^2 + \sin^2\theta\, d\varphi^2) \tag{6.187}$$

By the same procedure as above we find the radial coordinate velocity of light to be unity everywhere

$$\left(\frac{du}{dv}\right)^2 = 1 \tag{6.188}$$

so long as f^2 has no zeros. Thus in the u, v coordinates no natural boundary to light propagation can occur.

It is a simple task to obtain from (6.187) differential equations which lead to a transformation from r, t to u, v coordinates and a nonzero function f. The angular coordinates θ and φ will not be changed. The fundamental transformation equation for the metric tensor,

$$g_{\alpha\beta} = \frac{\partial \hat{x}^\mu}{\partial x^\alpha}\frac{\partial \hat{x}^\nu}{\partial x^\beta}\hat{g}_{\mu\nu} \tag{6.189}$$

and the line elements (6.53) and (6.187) lead to the following differential equations to be solved

$$\begin{aligned} 1 - \frac{2m}{r} &= f^2\left[\left(\frac{\partial v}{\partial x^0}\right)^2 - \left(\frac{\partial u}{\partial x^0}\right)^2\right] \\ -\left(1 - \frac{2m}{r}\right)^{-1} &= f^2\left[\left(\frac{\partial v}{\partial r}\right)^2 - \left(\frac{\partial u}{\partial r}\right)^2\right] \qquad x^0 = ct \\ 0 &= \frac{\partial u}{\partial x^0}\frac{\partial u}{\partial r} - \frac{\partial v}{\partial x^0}\frac{\partial v}{\partial r} \end{aligned} \tag{6.190}$$

Note that the signs of u and v are not determined by these equations. To simplify we introduce a new radial parameter ξ and a function $F(\xi)$ by

$$\xi = r + 2m \log\left|\frac{r}{2m} - 1\right| \tag{6.191}$$

$$F(\xi) = \frac{1 - 2m/r}{f^2(r)}$$

We have here assumed that a function f may be found which depends only on r; this is a critical point since an infinite number of transformations could lead to the metric form (6.187), and only this assumption leads to the Kruskal form and also removes the coordinate singularity

at $r = 2m$. The relations (6.190) now simplify to

$$\left(\frac{\partial v}{\partial x^0}\right)^2 - \left(\frac{\partial u}{\partial x^0}\right)^2 = F(\xi) \tag{6.192a}$$

$$\left(\frac{\partial v}{\partial \xi}\right)^2 - \left(\frac{\partial u}{\partial \xi}\right)^2 = -F(\xi) \tag{6.192b}$$

$$\frac{\partial u}{\partial x^0}\frac{\partial u}{\partial \xi} = \frac{\partial v}{\partial x^0}\frac{\partial v}{\partial \xi} \tag{6.192c}$$

If we add Eqs. (6.192*a*) and (6.192*b*) and alternately add or subtract twice (6.192*c*), we obtain

$$\left(\frac{\partial v}{\partial x^0} + \frac{\partial v}{\partial \xi}\right)^2 = \left(\frac{\partial u}{\partial x^0} + \frac{\partial u}{\partial \xi}\right)^2 \tag{6.193a}$$

$$\left(\frac{\partial v}{\partial x^0} - \frac{\partial v}{\partial \xi}\right)^2 = \left(\frac{\partial u}{\partial x^0} - \frac{\partial u}{\partial \xi}\right)^2 \tag{6.193b}$$

Using a relative plus sign for the roots of (6.193*a*) and a relative minus sign for the roots of (6.193*b*), we then obtain two equations (if we were to use the same sign, the Jacobian of the transformation would vanish):

$$\frac{\partial v}{\partial x^0} = \frac{\partial u}{\partial \xi} \qquad \frac{\partial v}{\partial \xi} = \frac{\partial u}{\partial x^0} \tag{6.194}$$

which lead to

$$\frac{\partial^2 u}{\partial x^{0^2}} - \frac{\partial^2 u}{\partial \xi^2} = 0 \qquad \frac{\partial^2 v}{\partial x^{0^2}} - \frac{\partial^2 v}{\partial \xi^2} = 0 \tag{6.195}$$

Thus both u and v satisfy the wave equation in x^0 and ξ. [If we had chosen the opposite roots in (6.193), the same equation (6.195) would have resulted.]

The general solution of the wave equation is an arbitrary twice-differentiable function of $x^0 \pm \xi$. Thus the solutions to (6.194) and (6.195) are easily seen to be

$$\begin{aligned} v &= h(\xi + x^0) + g(\xi - x^0) \\ u &= h(\xi + x^0) - g(\xi - x^0) \end{aligned} \tag{6.196}$$

where h and g are to be determined. Now we substitute u and v from (6.196) back into Eqs. (6.192); Eq. (6.192*c*) is automatically satisfied

while (6.192*a*) and (6.192*b*) are equivalent and lead to

$$-4h'(\xi + x^0)g'(\xi - x^0) = F(\xi) \tag{6.197}$$

where a prime indicates differentiation with respect to the argument. This is a remarkable equation that will lead to solutions for h, g, and F that are unique up to unimportant constants.

So far we have made no restrictions on the range of r in our transformation. Now we must specify whether r is greater than or less than $2m$, since in the two regions we shall have different transformation functions which must be patched together at the boundary. We first consider $r \geq 2m$, in which case F is positive from (6.191). To solve (6.197) we differentiate with respect to ξ and x^0 to obtain

$$\frac{F'(\xi)}{F(\xi)} = \frac{h''(\xi + x^0)}{h'(\xi + x^0)} + \frac{g''(\xi - x^0)}{g'(\xi - x^0)} \tag{6.198a}$$

$$0 = \frac{h''(\xi + x^0)}{h'(\xi + x^0)} - \frac{g''(\xi - x^0)}{g'(\xi - x^0)} \tag{6.198b}$$

Thus

$$[\log F(\xi)]' = 2[\log h(\xi + x^0)]' \tag{6.199}$$

We may treat ξ and $y \equiv \xi + x^0$ as independent variables, which implies that the two sides of (6.199) are functions of two independent variables and must both be equal to some constant η. Thus from (6.199) and (6.198*b*) we see that h, g, and F are exponential functions. We therefore write the solution to (6.197) as

$$h(y) = \tfrac{1}{2}e^{\eta y} \qquad g(y) = -\tfrac{1}{2}e^{\eta y} \qquad F(\xi) = \eta^2 e^{2\eta\xi} \tag{6.200}$$

where the arbitrary additive constants are chosen to be zero and the multiplicative constants to be $\frac{1}{2}$ for convenience. Note that the relative sign of h and g is negative, as dictated by $F > 0$. Now from (6.191), (6.196), and (6.200) we have the transformation

$$u = \left(\frac{r}{2m} - 1\right)^{2m\eta} e^{\eta r} \cosh \eta x^0$$

$$v = \left(\frac{r}{2m} - 1\right)^{2m\eta} e^{\eta r} \sinh \eta x^0 \tag{6.201}$$

$$f^2 = \frac{2m}{\eta^2 r}\left(\frac{r}{2m} - 1\right)^{1-4m\eta} e^{-2\eta r}$$

It remains only to choose the arbitrary parameter η; to do this we demand that f^2 have no zero or singularity at $r = 2m$, which requires that $\eta = 1/4m$. (Then ds^2 will vanish *only* on the light cone.) The transformation is thus, finally,

$$u = \sqrt{\frac{r}{2m} - 1}\, e^{r/4m} \cosh \frac{x^0}{4m}$$

$$v = \sqrt{\frac{r}{2m} - 1}\, e^{r/4m} \sinh \frac{x^0}{4m} \tag{6.202}$$

$$f^2 = \frac{32m^3}{r} e^{-r/2m} \qquad \to 0$$

à l'infini !

The region of the uv plane defined by (6.202) for $r \geq 2m$ is $u \geq |v|$, which is labeled O in Fig. 6.3. Some special lines are of interest; for any finite x^0 the boundary line $r = 2m$ in the rt plane corresponds to the point $u = v = 0$ in the uv plane. Also we note that $x^0 \to \infty$ corresponds to $u = v$ and $x^0 \to -\infty$ corresponds to $u = -v$ for any value of $r > 2m$. For other points in O we invert the transformation (6.202)

$$u^2 - v^2 = \left(\frac{r}{2m} - 1\right) e^{r/2m} \qquad \frac{v}{u} = \tanh \frac{x^0}{4m} \tag{6.203}$$

Thus lines of constant r and lines of constant x^0 form a mesh of intersecting hyperbolas and rays in O as shown in Fig. 6.3. As r approaches

Fig. 6.3
Kruskal coordinates with several lines of constant r and t shown. The regions O and O' correspond to $r > 2m$, while I and I' correspond to $r < 2m$.

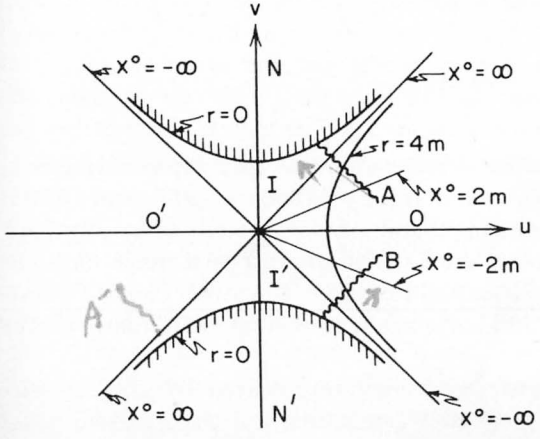

2m si on veut que f soit régulier il faut prendre eta = 4m et on joue alors «propriété» zéro puissance zéro = 1 !!!

spread them out into a line in a new $(r_{\text{new}}, t_{\text{new}})$-plane; and will squeeze the "line" ($r = 2M$, t from $-\infty$ to $+\infty$) into a single point in the $(r_{\text{new}}, t_{\text{new}})$-plane. One is the more prepared to accept this tentative conclusion and act on it because one has already seen (equation 31.8) that the region covering the (θ, ϕ) 2-sphere at $r = 2M$, and extending from $t = -\infty$ to $t = +\infty$, has zero proper volume. What timelier indication could one want that the "line" $r = 2M$, $-\infty < t < \infty$, is actually a point?

§31.4. SEVERAL WELL-BEHAVED COORDINATE SYSTEMS

Novikov coordinates: (1) how constructed

The well-behaved coordinate system that is easiest to visualize is one in which the radially moving test particles of equations (31.10) remain always at rest ("comoving coordinates"). Such coordinates were first used by Novikov (1963). Novikov attaches a specific value of his radial coordinate, R^*, to each test particle as it emerges from the singularity of infinite tidal forces at $r = 0$, and insists that the particle carry that value of R^* throughout its "cycloidal life"—up through $r = 2M$ to $r = r_{\max}$, then back down through $r = 2M$ to $r = 0$. For definiteness, Novikov expresses the R^* value for each particle in terms of the peak point on its trajectory by

$$R^* = (r_{\max}/2M - 1)^{1/2}. \tag{31.11}$$

As a time coordinate, Novikov uses proper time τ of the test particles, normalized so $\tau = 0$ at the peak of the orbit. Every particle in the swarm is ejected in such a manner that it arrives at the summit of its trajectory ($r = r_{\max}$, $\tau = 0$) at one and the same value of the Schwarzschild coordinate time; namely, at $t = 0$.

Simple though they may be conceptually, the Novikov coordinates are related to the original Schwarzschild coordinates by a very complicated transformation: (1) combine equations (31.10b) and (31.11) to obtain $\eta(\tau, R^*)$; (2) combine $\eta(\tau, R^*)$ with (31.10a) and (31.11) to obtain $r(\tau, R^*)$; (3) combine $\eta(\tau, R^*)$ with (31.10c) and (31.11) to obtain $t(\tau, R^*)$. The resulting coordinate transformation, when applied to the Schwarzschild metric (31.1), yields the line element

(2) line element

$$ds^2 = -d\tau^2 + \left(\frac{R^{*2}+1}{R^{*2}}\right)\left(\frac{\partial r}{\partial R^*}\right)^2 dR^{*2} + r^2(d\theta^2 + \sin^2\theta\, d\phi^2). \tag{31.12a}$$

("*Schwarzschild geometry in Novikov coordinates*".) Here r is no longer a radial coordinate; it is now a metric function $r(\tau, R^*)$ given implicitly by

$$\frac{\tau}{2M} = \pm (R^{*2}+1)\left[\frac{r}{2M} - \frac{(r/2M)^2}{R^{*2}+1}\right]^{1/2} + (R^{*2}+1)^{3/2}\cos^{-1}\left[\left(\frac{r/2M}{R^{*2}+1}\right)^{1/2}\right]. \tag{31.12b}$$

Figure 31.2 shows the locations of several key regions of Schwarzschild spacetime in this coordinate system. The existence of two distinct regions with $r = 0$ (singularities) and two distinct regions with $r \longrightarrow \infty$ (asymptotically flat regions; recall that $4\pi r^2$ = surface area!) will be discussed in §31.5.

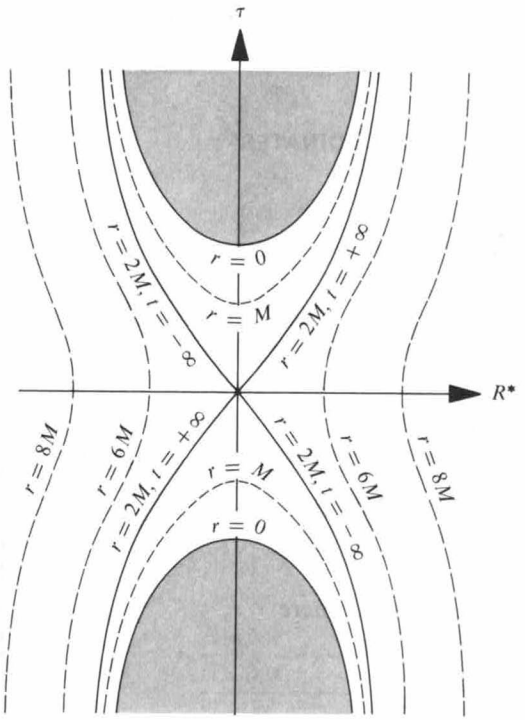

Figure 31.2.
The Novikov coordinate system for Schwarzschild spacetime (schematic). The dashed curves are curves of constant r (recall: $4\pi r^2$ = surface area about center of symmetry). The region shaded gray is not part of spacetime; it corresponds to $r < 0$, a region that cannot be reached because of the singularity of spacetime at $r = 0$. Notice that the "line" ($r = 2M$, $-\infty < t < +\infty$) of the Schwarzschild coordinate diagram (Figure 31.1) has been compressed into a point here, in accordance with the discussion at the end of §31.3.

Although Novikov's coordinate system is very simple conceptually, the mathematical expressions for the metric components in it are rather unwieldy. Simpler, more usable expressions have been obtained in a different coordinate system ("Kruskal-Szekeres coordinates") by Kruskal (1960), and independently by Szekeres (1960).

Kruskal-Szekeres coordinates

Kruskal and Szekeres use a dimensionless radial coordinate u and a dimensionless time coordinate v related to the Schwarzschild r and t by

$$\left.\begin{aligned} u &= (r/2M - 1)^{1/2} e^{r/4M} \cosh(t/4M) \\ v &= (r/2M - 1)^{1/2} e^{r/4M} \sinh(t/4M) \end{aligned}\right\} \text{ when } r > 2M, \tag{31.13a}$$

$$\left.\begin{aligned} u &= (1 - r/2M)^{1/2} e^{r/4M} \sinh(t/4M) \\ v &= (1 - r/2M)^{1/2} e^{r/4M} \cosh(t/4M) \end{aligned}\right\} \text{ when } r < 2M. \tag{31.13b}$$

(Motivation for introducing such coordinates is given in Box 31.2.) By making this change of coordinates in the Schwarzschild metric (31.1), one obtains the following line element:

$$ds^2 = (32M^3/r)e^{-r/2M}(-dv^2 + du^2) + r^2(d\theta^2 + \sin^2\theta\, d\phi^2) \tag{31.14a}$$

("*Schwarzschild geometry in Kruskal-Szekeres coordinates*"). Here r is to be regarded as a function of u and v defined implicitly by

$$(r/2M - 1)e^{r/2M} = u^2 - v^2 \tag{31.14b}$$

[cf. equations (31.13)].

(*continued on page 833*)

Box 31.2 MOTIVATION FOR KRUSKAL-SZEKERES COORDINATES*

A. EDDINGTON-FINKELSTEIN COORDINATES

The motivation for the Kruskal-Szekeres system begins by introducing a different coordinate system, first devised by Eddington (1924) and rediscovered by Finkelstein (1958). Eddington and Finkelstein use as the foundation of their coordinate system, not freely falling particles as did Novikov, but freely falling photons. More particularly, they introduce coordinates $\tilde{U}$ and $\tilde{V}$, which are labels for outgoing and ingoing, radial, null geodesics. The geodesics are given by

$$ds^2 = 0 = -(1 - 2M/r)\,dt^2 + (1 - 2M/r)^{-1}\,dr^2.$$

Equivalently, outgoing geodesics are given by $\tilde{U} = \text{const}$, where

$$\tilde{U} \equiv t - r^*; \tag{1a}$$

and ingoing geodesics are given by $\tilde{V} = \text{const}$, where

$$\tilde{V} \equiv t + r^*. \tag{1b}$$

Here r^* is the "tortoise coordinate" of §25.5 and Figure 25.4:

$$r^* \equiv r + 2M \ln|r/2M - 1|. \tag{1c}$$

alias la coordonnée ξ dans Adler Schiffer Bazin equation 6.191

Ingoing Eddington-Finkelstein Coordinates—Adopt r and $\tilde{V}$ as coordinates in place of r and t

mais le détail du calcul n'est pas donné

The Schwarzschild metric becomes.

$$ds^2 = -(1 - 2M/r)\,d\tilde{V}^2 + 2\,d\tilde{V}\,dr + r^2\,d\Omega^2. \tag{2}$$

The radial light cone, $ds^2 = 0$, has one leg

$$d\tilde{V}/dr = 0, \tag{3a}$$

and the other leg

$$\frac{d\tilde{V}}{dr} = \frac{2}{1 - 2M/r}. \tag{3b}$$

From this, and this alone, one can infer all features of the drawing.

*This box is based on Misner (1969a).

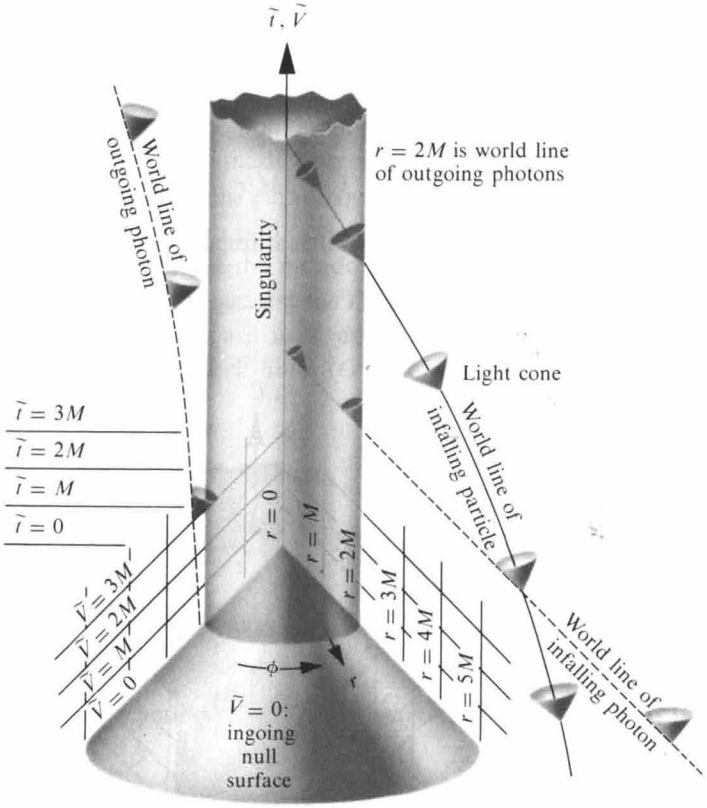

Ingoing Eddington-Finkelstein coordinates (one rotational degree of freedom is suppressed; i.e., θ is set equal to $\pi/2$). Surfaces of constant $\tilde{V}$, being ingoing null surfaces, are plotted on a 45-degree slant, just as they would be in flat spacetime. Equivalently, surfaces of constant

$$\tilde{t} \equiv \tilde{V} - r = t + 2M \ln |r/2M - 1|$$

are plotted as horizontal surfaces.

Outgoing Eddington-Finkelstein Coordinates—Adopt r and $\tilde{U}$ as coordinates in place of r and t

The Schwarzschild metric becomes

$$ds^2 = -(1 - 2M/r)\, d\tilde{U}^2 - 2\, d\tilde{U}\, dr + r^2\, d\Omega^2. \tag{4}$$

Box 31.2 (*continued*)

The radial light cone, $ds^2 = 0$, has one leg

$$d\tilde{U}/dr = 0, \tag{5a}$$

and the other leg

$$\frac{d\tilde{U}}{dr} = -\frac{2}{1 - 2M/r}. \tag{5b}$$

From this, and this alone, one can infer all features of the drawing.

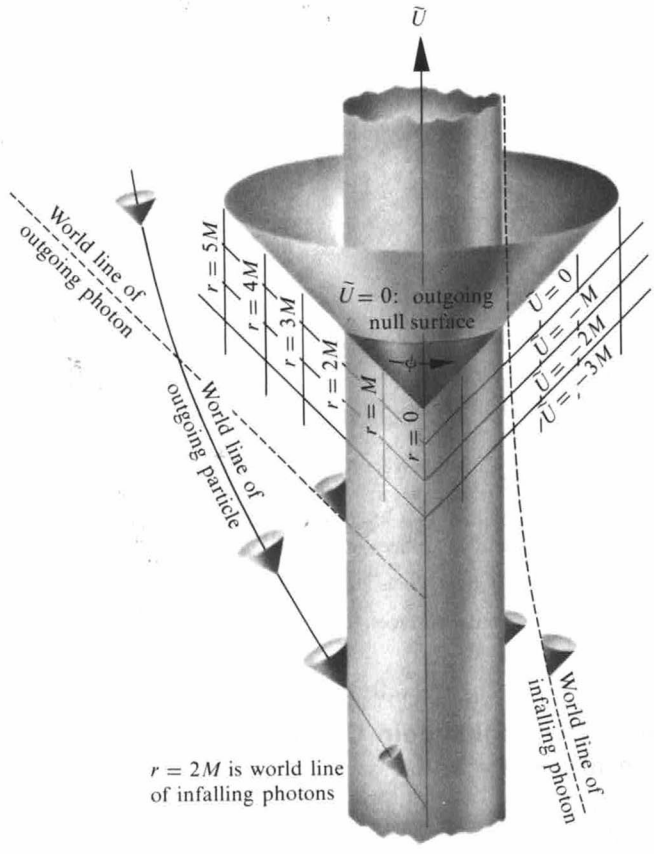

Outgoing Eddington-Finkelstein coordinates (one rotational degree of freedom is suppressed). (Surfaces of constant $\tilde{U}$, being outgoing null surfaces, are plotted on a 45-degree slant, just as they would be in flat spacetime.)

Notice that both Eddington-Finkelstein coordinate systems are better behaved at the gravitational radius than is the Schwarzschild coordinate system; but they are not *fully* well-behaved. The outgoing coordinates $(\tilde{U}, r, \theta, \phi)$ describe in a non-pathological manner the ejection of particles outward from $r = 0$ through $r = 2M$; but their description of infall through $r = 2M$ has the same pathology as the description given by Schwarzschild coordinates (Figure 31.1). Similarly, the ingoing coordinates $(\tilde{V}, r, \theta, \phi)$ describe well the infall of a particle through $r = 2M$, but they give a pathological description of outgoing trajectories. Moreover, the contrast between the two diagrams seems paradoxical: in one the gravitational radius is made up of world lines of outgoing photons; in the other it is made up of world lines of ingoing photons! To resolve the paradox, one must seek another, better-behaved coordinate system. [But *note:* because the ingoing Eddington-Finklestein coordinates describe infall so well, they are used extensively in discussions of gravitational collapse (Chapter 32) and black holes (Chapters 33 and 34).]

B. TRANSITION FROM EDDINGTON-FINKELSTEIN TO KRUSKAL-SZEKERES

Perhaps one would obtain a fully well-behaved coordinate system by dropping r from view and using $\tilde{U}$, $\tilde{V}$, as the two coordinates in the radial-time plane. The resulting coordinate system is related to Schwarzschild coordinates by [see equations (1)]

$$\tilde{V} - \tilde{U} = 2r^*, \tag{6a}$$

$$\tilde{V} + \tilde{U} = 2t; \tag{6b}$$

and the line element in terms of the new coordinates reads

$$ds^2 = -(1 - 2M/r)\, d\tilde{U}\, d\tilde{V} + r^2(d\theta^2 + \sin^2\theta\, d\phi^2). \tag{7}$$

Contrary to one's hopes, this coordinate system is pathological at $r = 2M$.

Second thoughts about the construction reveal the trouble: the surfaces $\tilde{U} =$ constant (outgoing null surfaces) used in constructing it are geometrically well-defined, as are the surfaces $\tilde{V} =$ constant (ingoing null surfaces); but the way of labeling them is not. Any relabeling, $\bar{u} = F(\tilde{U})$ and $\bar{v} = G(\tilde{V})$, will leave the surfaces unchanged physically. What one needs is a relabeling that will get rid of the singular factor $1 - 2M/r$ in the line element (7). A successful relabeling is suggested by the equation

$$\exp[(\tilde{V} - \tilde{U})/4M] = \exp(r^*/2M) = (r/2M - 1)\exp(r/2M), \tag{8}$$

Box 31.2 (*continued*)

which follows from equations (6a) and (1c). Experimenting with this relation quickly reveals that the relabeling

$$\tilde{u} \equiv -e^{-\tilde{U}/4M} = -(r/2M - 1)^{1/2} e^{r/4M} e^{-t/4M}, \tag{9a}$$

$$\tilde{v} \equiv e^{+\tilde{V}/4M} = (r/2M - 1)^{1/2} e^{r/4M} e^{t/4M}, \tag{9b}$$

will remove the offending $1 - 2M/r$ from the metric coefficients. In terms of these new coordinates, the line element reads

$$ds^2 = -(32M^3/r) e^{-r/2M}\, d\tilde{v}\, d\tilde{u} + r^2(d\theta^2 + \sin^2\theta\, d\phi^2). \tag{10a}$$

Here r is still defined by $4\pi r^2 =$ surface area, but it must be regarded as a function of $\tilde{v}$ and $\tilde{u}$:

$$(r/2M - 1) e^{r/2M} = -\tilde{u}\tilde{v}. \tag{10b}$$

One can readily verify that this equation determines r uniquely (recall: $r > 0$!) in terms of the product $\tilde{u}\tilde{v}$ [details in Misner (1969a)].

The coordinates, $\tilde{u}$, $\tilde{v}$, which label the ingoing and outgoing null surfaces, are null coordinates; i.e.,

$$\partial/\partial\tilde{u} \cdot \partial/\partial\tilde{u} = g_{\tilde{u}\tilde{u}} = 0, \qquad \partial/\partial\tilde{v} \cdot \partial/\partial\tilde{v} = g_{\tilde{v}\tilde{v}} = 0$$

[see equation (10a)]. If one is not accustomed to working with null coordinates, it is helpful to replace $\tilde{u}$ and $\tilde{v}$ by spacelike and timelike coordinates, u and v (Kruskal-Szekeres coordinates!) defined by

$$u \equiv \frac{1}{2}(\tilde{v} - \tilde{u}) = (r/2M - 1)^{1/2} e^{r/4M} \cosh(t/4M), \tag{11a}$$

$$v \equiv \frac{1}{2}(\tilde{v} + \tilde{u}) = (r/2M - 1)^{1/2} e^{r/4M} \sinh(t/4M), \tag{11b}$$

so that

$$dv^2 - du^2 = d\tilde{v}\, d\tilde{u}. \tag{12}$$

In terms of these coordinates, the line element has the Kruskal form (31.14), which is fully well-behaved at the gravitational radius.

Although the Kruskal-Szekeres line element is well behaved at $r = 2M$, the transformation (11) from Schwarzschild to Kruskal-Szekeres is not; it becomes meaningless (u and v "imaginary") when one moves from $r > 2M$ to $r < 2M$. Of course, this is a manifestation of the pathologies of Schwarzschild coordinates. By trial and error, one readily finds a new transformation, to replace (11) at $r < 2M$, leading from Schwarzschild to Kruskal-Szekeres coordinates:

$$u = (1 - r/2M)^{1/2} e^{r/4M} \sinh(t/4M), \tag{11c}$$

$$v = (1 - r/2M)^{1/2} e^{r/4M} \cosh(t/4M). \tag{11d}$$

§31.5. RELATIONSHIP BETWEEN KRUSKAL-SZEKERES COORDINATES AND SCHWARZSCHILD COORDINATES

Kruskal-Szekeres coordinates reveal that Schwarzschild spacetime has two "$r = 0$ singularities" and two "$r \longrightarrow \infty$ exterior regions"

In the Kruskal-Szekeres coordinate system, the singularity $r = 0$ is located at $v^2 - u^2 = 1$. Thus there are actually *two* singularities, not one; both

$$v = +(1 + u^2)^{1/2} \text{ and } v = -(1 + u^2)^{1/2} \text{ correspond to } r = 0! \qquad (31.15)$$

This is not the only surprise that lies hidden in the Kruskal-Szekeres line element (31.14). Notice also that $r \gg 2M$ (the region of spacetime far outside the gravitational radius) is given by $u^2 \gg v^2$. Thus there are actually *two* exterior regions*; both

$$u \gg +|v| \text{ and } u \ll -|v| \text{ correspond to } r \gg 2M! \qquad (31.16)$$

How can this be? When the geometry is charted in Schwarzschild coordinates, it contains one singularity and one exterior region; but when expressed in Kruskal-Szekeres coordinates, it shows two of each. The answer must be that the Schwarzschild coordinates cover only part of the spacetime manifold; they must be only a local coordinate patch on the full manifold. Somehow, by means of the coordinate transformation that leads to Kruskal-Szekeres coordinates, one has analytically extended the limited Schwarzschild solution for the metric to cover all (or more nearly all) of the manifold.

To understand this covering more clearly, transform back from Kruskal-Szekeres coordinates to Schwarzschild coordinates (see Figure 31.3). The transformation equations, as written down in (31.13) were valid only for the quadrants $u > |v|$ [equation (31.13a)] and $v > |u|$ [equation (31.13b)] of Kruskal coordinates. Denote these quadrants by the numerals I and II; and denote the other quadrants by III and IV (see Figure 31.3). In the other quadrants, one can also transform the Kruskal-Szekeres line element (31.14) into the Schwarzschild line element (31.1); but slightly different transformation equations are needed. One easily verifies that the following sets of transformations work:

Transformation between Schwarzschild coordinates and Kruskal-Szekeres coordinates

$$\text{(I)} \quad \begin{cases} u = (r/2M - 1)^{1/2} e^{r/4M} \cosh(t/4M) \\ v = (r/2M - 1)^{1/2} e^{r/4M} \sinh(t/4M) \end{cases}, \qquad (31.17a)$$

$$\text{(II)} \quad \begin{cases} u = (1 - r/2M)^{1/2} e^{r/4M} \sinh(t/4M) \\ v = (1 - r/2M)^{1/2} e^{r/4M} \cosh(t/4M) \end{cases}, \qquad (31.17b)$$

$$\text{(III)} \quad \begin{cases} u = -(r/2M - 1)^{1/2} e^{r/4M} \cosh(t/4M) \\ v = -(r/2M - 1)^{1/2} e^{r/4M} \sinh(t/4M) \end{cases}, \qquad (31.17c)$$

$$\text{(IV)} \quad \begin{cases} u = -(1 - r/2M)^{1/2} e^{r/4M} \sinh(t/4M) \\ v = -(1 - r/2M)^{1/2} e^{r/4M} \cosh(t/4M) \end{cases}. \qquad (31.17d)$$

*The global structure of the Schwarzschild geometry, including the existence of two singularities and two exterior regions, was first discovered by Synge (1950). See Box 31.1.

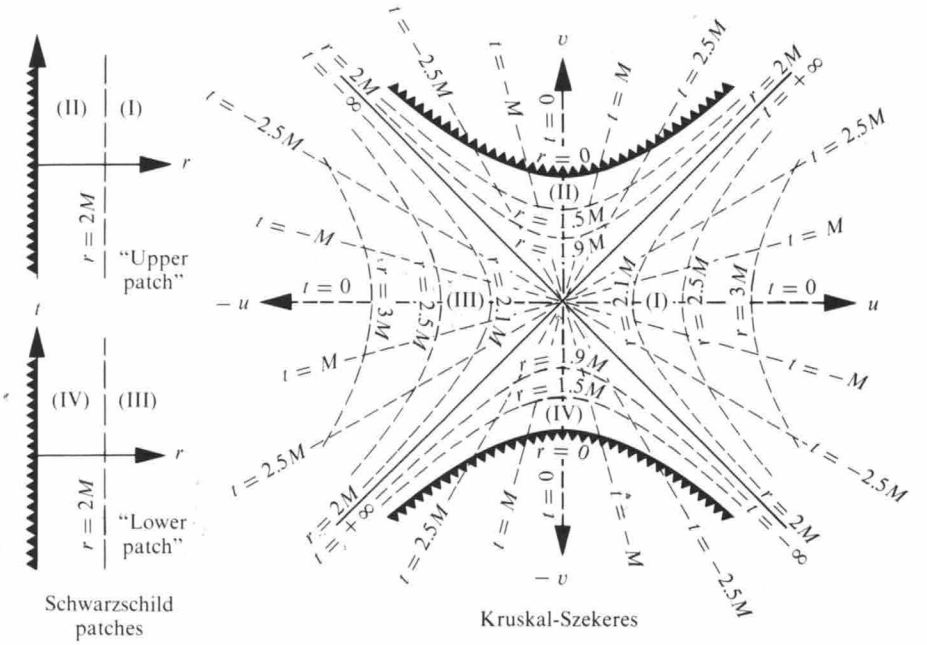

Figure 31.3.
The transformation of the Schwarzschild vacuum geometry between Schwarzschild and Kruskal-Szekeres coordinates. Two Schwarzschild coordinate patches I, II, and III, IV (illustrated in the upper and lower portions of Figure 31.5,a) are required to cover the complete Schwarzschild geometry, whereas a single Kruskal-Szekeres coordinate system suffices. The Schwarzschild geometry consists of four regions I, II, III, IV. Regions I and III represent two distinct, but identical, asymptotically flat universes in which $r > 2M$; while regions II and IV are two identical, but time-reversed, regions in which physical singularities ($r = 0$) evolve. The transformation laws that relate the Schwarzschild and Kruskal-Szekeres coordinate systems to each other are given by equations (31.17) and (31.18). In the Kruskal-Szekeres u,v-plane, curves of constant r are hyperbolae with asymptotes $u = \pm v$, while curves of constant t are straight lines through the origin.

The inverse transformations are

$$(r/2M - 1)e^{r/2M} = u^2 - v^2 \text{ in I, II, III, IV;} \tag{31.18a}$$

$$t = \begin{cases} 4M \tanh^{-1}(v/u) \text{ in I and III,} \\ 4M \tanh^{-1}(u/v) \text{ in II and IV.} \end{cases} \tag{31.18b}$$

Two Schwarzschild coordinate patches are required to cover all of spacetime

These coordinate transformations are exhibited graphically in Figure 31.3. Notice that two Schwarzschild coordinate patches, I, II, and III, IV, are required to cover the entire Schwarzschild geometry; but a single Kruskal coordinate system suffices. Schwarzschild patch I, II, is divided into two regions—region I, which is outside the gravitational radius ($r > 2M$), and region II, which is inside the gravitational radius ($r < 2M$). Similarly, Schwarzschild patch III, IV, consists of an exterior region (III) and an interior region (IV).

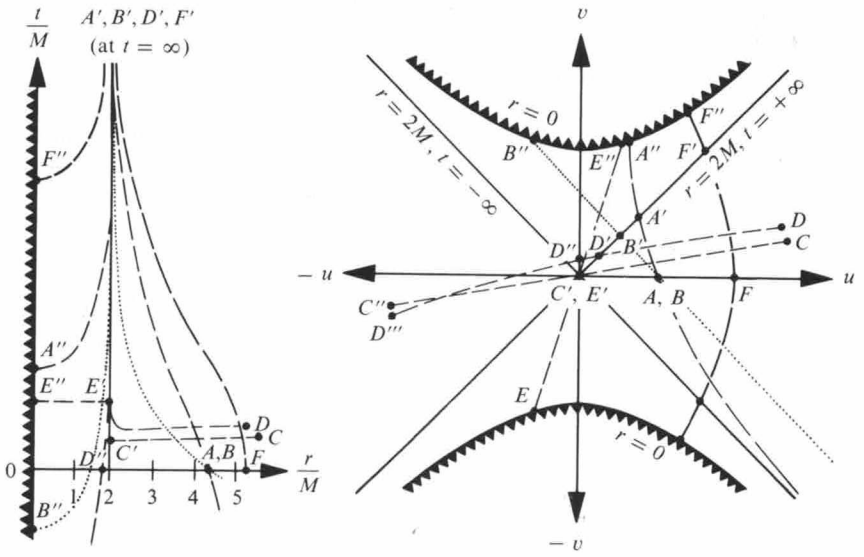

(a) Schwarzschild

(b) Kruskal-Szekeres

Figure 31.4.

(a) Typical radial timelike (A, E, F), lightlike (B), and spacelike (C, D) geodesics of the Schwarzschild geometry, as seen in the Schwarzschild coordinate system (schematic only). This is a reproduction of Figure 31.1.

(b) The same geodesics, as seen in the Kruskal-Szekeres coordinate system, and as extended either to infinite length or to the singularity of infinite curvature at $r = 0$ (schematic only).

Equations (31.18) reveal that the regions of constant r (constant surface area) are hyperbolae with asymptotes $u = \pm v$ in the Kruskal-Szekeres diagram, and that regions of constant t are straight lines through the origin.

Properties of the Kruskal-Szekeres coordinate system

Several radial geodesics of the complete Schwarzschild geometry are depicted in the Kruskal-Szekeres coordinate system in Figure 31.4. Notice how much more reasonable the geodesic curves look in Kruskal-Szekeres coordinates than in Schwarzschild coordinates. Notice also that *radial, lightlike geodesics (paths of radial light rays) are 45-degree lines in the Kruskal-Szekeres coordinate system.* This can be seen from the Kruskal-Szekeres line element (31.14), for which $du = \pm dv$ guarantees $ds = 0$. Because of this 45-degree property, the radial light cone in a Kruskal-Szekeres diagram has the same form as in the space-time diagram of special relativity. Any radial curve that points "generally upward" (i.e., makes an angle of less than 45 degrees with the vertical, v, axis) is timelike; and curves that point "generally outward" are spacelike. This property enables a Kruskal-Szekeres diagram to exhibit easily the causality relation between one event in spacetime and another (see exercises 31.2 to 31.4).

EXERCISES

Exercise 31.2. NONRADIAL LIGHT CONES

Show that the world line of a photon traveling nonradially makes an angle less than 45 degrees with the vertical v-axis of a Kruskal-Szekeres coordinate diagram. From this, infer that particles with finite rest mass, traveling nonradially or radially, must always move "generally upward" (angle less than 45 degrees with vertical v-axis).

Exercise 31.3. THE CRACK OF DOOM

Use a Kruskal diagram to show the following.

(a) If a man allows himself to fall through the gravitational radius $r = 2M$, there is no way whatsoever for him to avoid hitting (and being killed in) the singularity at $r = 0$.

(b) Once a man has fallen inward through $r = 2M$, there is no way whatsoever that he can send messages out to his friends at $r > 2M$, but he can still receive messages from them (e.g., by radio waves, or laser beam, or infalling "CARE packages").

Exercise 31.4. HOW LONG TO LIVE?

Show that once a man falling inward reaches the gravitational radius, no matter what he does subsequently (no matter in what directions, how long, and how hard he blasts his rocket engines), he will be pulled into the singularity and killed in a proper time of

$$\tau < \tau_{\max} = \pi M = 1.54 \times 10^{-5}(M/M_{\odot}) \text{ seconds.} \tag{31.19}$$

[*Hint:* The trajectory of longest proper time lapse must be a geodesic. Use the mathematical tools of Chapter 25 to show that the geodesic of longest proper time lapse between $r = 2M$ and $r = 0$ is the radial geodesic (31.10a), with $r_{\max} = 2M$, for which the time lapse is πM.]

Exercise 31.5. EDDINGTON-FINKELSTEIN AND KRUSKAL-SZEKERES COMPARED

Use coordinate diagrams to compare the ingoing and outgoing Eddington-Finkelstein coordinates of Box 31.2 with the Kruskal-Szekeres coordinates. Pattern the comparison after that between Schwarzschild and Kruskal-Szekeres in Figures 31.3 and 31.4.

Exercise 31.6. ANOTHER COORDINATE SYSTEM

Construct a coordinate diagram for the $\tilde{U}$, $\tilde{V}$, θ, ϕ coordinate system of Box 31.2 [equations (6) and (7)]. Show such features as (1) the relationship to Schwarzschild and to Kruskal-Szekeres coordinates; (2) the location of $r = 2M$; and (3) radial geodesics.

§31.6. DYNAMICS OF THE SCHWARZSCHILD GEOMETRY

What does the Schwarzschild geometry look like? This question is most readily answered by means of embedding diagrams analogous to those for an equilibrium star (§23.8; Figure 23.1; and end of Box 23.2) and for Friedmann universes of positive and negative spatial curvature [equations (27.23) and (27.24) and Box 27.2].

Examine, first, the geometry of the spacelike hypersurface $v = 0$, which extends from $u = +\infty$ ($r = \infty$) into $u = 0$ ($r = 2M$) and then out to $u = -\infty$ ($r = \infty$). In Schwarzschild coordinates this surface is a slice of constant time, $t = 0$ [see equation (31.18b)]; it is precisely the surface for which an embedding diagram was calculated in equation (23.34b). The embedded surface, with one degree of rotational freedom suppressed, is described by the paraboloid of revolution

$$\bar{r} = 2M + \bar{z}^2/8M \tag{31.20}$$

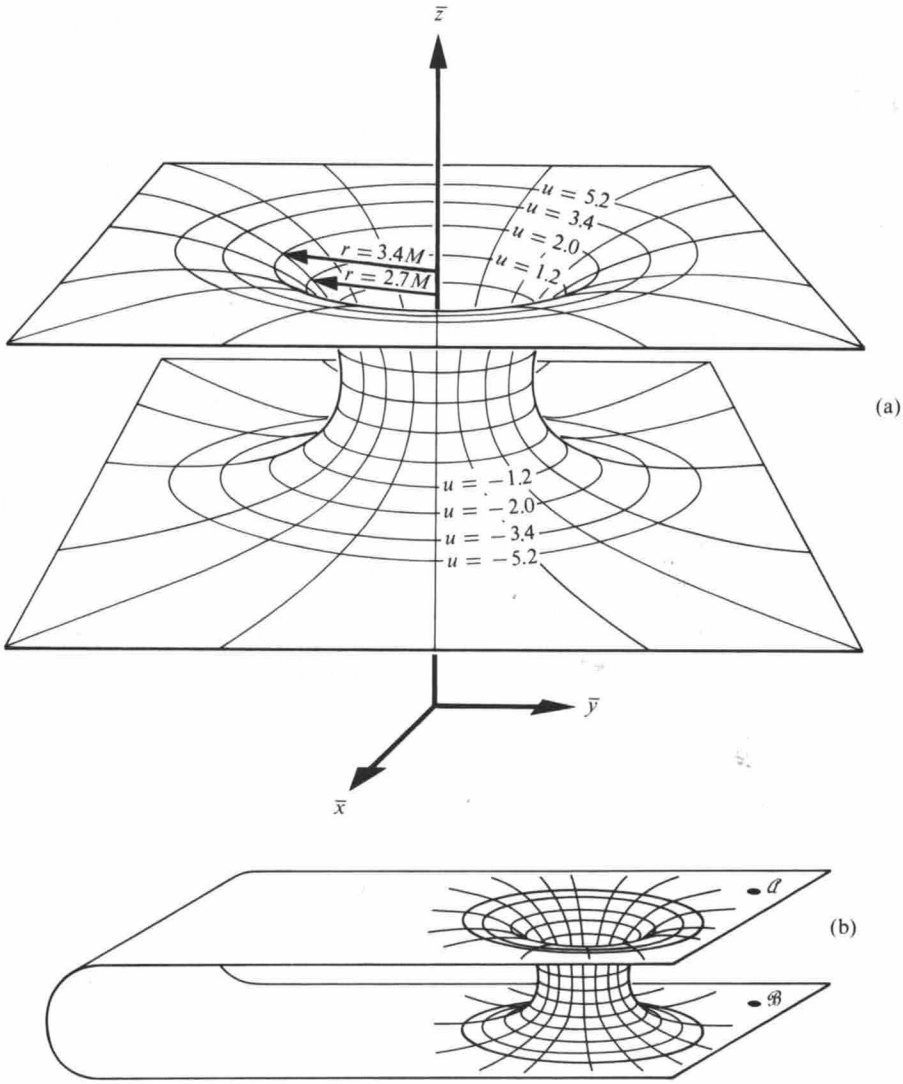

Figure 31.5.

(a) The Schwarzschild space geometry at the "moment of time" $t = v = 0$, with one degree of rotational freedom suppressed ($\theta \triangleq \pi/2$). To restore that rotational freedom and obtain the full Schwarzschild 3-geometry, one mentally replaces the circles of constant $\bar{r} = (\bar{x}^2 + \bar{y}^2)^{1/2}$ with spherical surfaces of area $4\pi\bar{r}^2$. Note that the resultant 3-geometry becomes flat (Euclidean) far from the throat of the bridge in both directions (both "universes").

(b) An embedding of the Schwarzschild space geometry at "time" $t = v = 0$, which is geometrically identical to the embedding (a), but which is topologically different. Einstein's field equations fix the local geometry of spacetime, but they do not fix its topology; see the discussion at end of Box 27.2. Here the Schwarzschild "wormhole" connects two distant regions of a single, asymptotically flat universe. For a discussion of issues of causality associated with this choice of topology, see Fuller and Wheeler (1962).

in the flat Euclidean space with metric

$$d\sigma^2 = d\bar{r}^2 + d\bar{z}^2 + \bar{r}^2\, d\bar{\phi}^2. \tag{31.21}$$

(See Figure 31.5.)

Notice from the embedding diagram of Figure 31.5,a, that the Schwarzschild

The 3-surface $v = t = 0$ is a "wormhole" connecting two asymptotically flat universes, or two different regions of one universe

geometry on the spacelike hypersurface $t = \text{const}$ consists of a bridge or "wormhole" connecting two distinct, but identical, asymptotically flat universes. This bridge is sometimes called the "Einstein-Rosen bridge" and sometimes the "Schwarzschild throat" or the "Schwarzschild wormhole." If one so wishes, one can change the topology of the Schwarzschild geometry by connecting the two asymptotically flat universes together in a region distant from the Schwarzschild throat [Fuller and Wheeler (1962); Fig. 31.5b]. The single, unique universe then becomes multiply connected, with the Schwarzschild throat providing one spacelike path from point $\mathcal{A}$ to point $\mathcal{B}$, and the nearly flat universe providing another. For concreteness, focus attention on the interpretation of the Schwarzschild geometry, not in terms of Wheeler's multiply connected single universe, but rather in terms of the Einstein-Rosen double universe of Figure 31.5,a.

Schwarzschild geometry is dynamic in regions $r < 2M$

One is usually accustomed to think of the Schwarzschild geometry as static. However, the static "time translations," $t \longrightarrow t + \Delta t$, which leave the Schwarzschild geometry unchanged, are time translations in the strict sense of the words only in regions I and III of the Schwarzschild geometry. In regions II and IV, $t \longrightarrow t + \Delta t$ is a spacelike motion, not a timelike motion (see Fig. 31.3). Consequently, a spacelike hypersurface, such as the surface $t = \text{const}$ of Figure 31.5,a, which extends from region I through $u = v = 0$ into region III, is *not* static. As this spacelike hypersurface is pushed forward in time (in the $+v$ direction of the Kruskal diagram), it enters region II, and its geometry begins to change.

In order to examine the time-development of the Schwarzschild geometry, one needs a sequence of embedding diagrams, each corresponding to the geometry of a spacelike hypersurface to the future of the preceding one. But how are the hypersurfaces to be chosen? In Newtonian theory or special relativity, one chooses hypersurfaces of constant time. But in dynamic regions of curved spacetime, no naturally preferred time coordinate exists. This situation forces one to make a totally *arbitrary* choice of hypersurfaces to use in visualizing the time-development of geometry, and to keep in mind how very arbitrary that choice was.

Time evolution of the wormhole: creation; expansion; recontraction; and pinch-off

Figure 31.6 uses two very different choices of hypersurfaces to depict the time-development of the Schwarzschild geometry. (Still other choices are shown in Figure 21.4.) Notice that the precise geometry of the evolving bridge depends on the arbitrary choice of spacelike hypersurfaces, but that the qualitative nature of the evolution is independent of the choice of hypersurfaces. Qualitatively speaking, the two asymptotically flat universes begin disconnected, with each one containing a singularity of infinite curvature ($r = 0$). As the two universes evolve in time, their singularities join each other and form a nonsingular bridge. The bridge enlarges, until it reaches a maximum radius at the throat of $r = 2M$ (maximum circumference of $4\pi M$; maximum surface area of $16\pi M^2$). It then contracts and pinches off, leaving the two universes disconnected and containing singularities ($r = 0$) once again. The formation, expansion, and collapse of the bridge occur so rapidly, that no particle or light ray can pass across the bridge from the faraway region of the one universe to the faraway region of the other without getting caught and crushed in the throat as it pinches off. (To verify this, examine the Kruskal-Szekeres diagram of Figure 31.3, where radial light rays move along 45-degree lines.)

Communication through the wormhole is impossible: it pinches off too fast

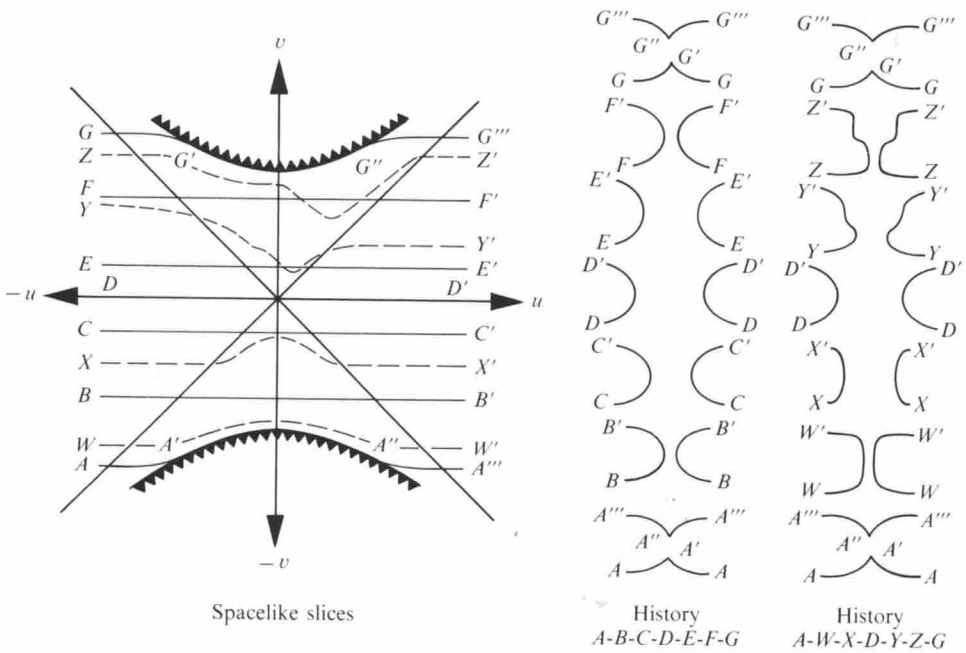

Figure 31.6.
Dynamical evolution of the Einstein-Rosen bridge of the vacuum Schwarzschild geometry (schematic). Shown here are two sequences of embedding diagrams corresponding to two different ways of viewing the evolution of the bridge—History *A-B-C-D-E-F-G*, and History *A-W-X-D-Y-Z-G*. The embedding diagrams are skeletonized in that each diagram must be rotated about the appropriate vertical axis in order to become two-dimensional surfaces analogous to Figure 31.5,a. [Notice that the hypersurfaces of which embedding diagrams are given intersect the singularity only tangentially. Hypersurfaces that intersect the singularity at a finite angle in the u,v-plane are not shown because they cannot be embedded in a Euclidean space. Instead, a Minkowski space (indefinite metric) must be used, at least near $r = 0$. For an example of an embedding in Minkowski space, see the discussion of a universe with constant negative spatial curvature in equations (27.23) and (27.24) and Box 27.2C.] Figure 21.4 exhibits embedding diagrams for other spacelike slices in the Schwarzschild geometry.

Creation and destruction in the singularities

From the Kruskal-Szekeres diagram and the 45-degree nature of its radial light rays, one sees that any particle that ever finds itself in region IV of spacetime must have been "created" in the earlier singularity; and any particle that ever falls into region II is doomed to be crushed in the later singularity. Only particles that stay forever in one of the asymptotically flat universes I or III, outside the gravitational radius ($r > 2M$), are forever safe from the singularities.

Nonviable proposals for modifying the topology of Schwarzschild spacetime

Some investigators, disturbed by the singularities at $r = 0$ or by the "double-universe" nature of the Schwarzschild geometry, have proposed modifications of its topology. One proposal is that the earlier and later singularities be identified with each other, so that a particle which falls into the singularity of region II, instead of being destroyed, will suddenly reemerge, being ejected, from the singularity of region IV. One cannot overstate the objections to this viewpoint: the region $r = 0$ is a physical singularity of infinite tidal gravitation forces and infinite Riemann curvature. Any particle that falls into that singularity must be destroyed by those

forces. Any attempt to extrapolate its fate through the singularity using Einstein's field equations must fail; the equations lose their predictive power in the face of infinite curvature. Consequently, to postulate that the particle reemerges from the earlier singularity is to make up an *ad hoc* mathematical rule, one unrelated to physics. It is conceivable, but few believe it true, that any object of finite mass will modify the geometry of the singularity as it approaches $r = 0$ to such an extent that it can pass through and reemerge. However, whether such a speculation is correct must be answered not by *ad hoc* rules, but by concrete, difficult computations within the framework of general relativity theory (see Chapter 34).

A second proposal for modifying the topology of the Schwarzschild geometry is this: one should avoid the existence of two different asymptotically flat universes by identifying each point (v, u, θ, ϕ) with its opposite point $(-v, -u, \theta, \phi)$ in the Kruskal-Szekeres coordinate system. Two objections to this proposal are: (1) it produces a sort of "conical" singularity (absence of local Lorentz frames) at $(v, u) = (0, 0)$, i.e., at the neck of the bridge at its moment of maximum expansion; and (2) it leads to causality violations in which a man can meet himself going backward in time.

One good way for the reader to become conversant with the basic features of the Schwarzschild geometry is to reread §§31.1–31.4 carefully, reinterpreting everything said there in terms of the Kruskal-Szekeres diagram.

EXERCISES

Exercise 31.7. SCHWARZSCHILD METRIC IN ISOTROPIC COORDINATES

(a) Show that, rewritten in the isotropic coordinates of Exercise 23.1, the Schwarzschild metric reads

$$ds^2 = -\left(\frac{1 - M/2\bar{r}}{1 + M/2\bar{r}}\right)^2 dt^2 + \left(1 + \frac{M}{2\bar{r}}\right)^4 [d\bar{r}^2 + \bar{r}^2(d\theta^2 + \sin^2\theta\, d\phi^2)]; \qquad (31.22)$$

and derive the transformation

$$r = \bar{r}(1 + M/2\bar{r})^2 \qquad (31.23)$$

between the two radial coordinates.

(b) Which regions of spacetime (I, II, III, IV; see Figure 31.3) are covered by the isotropic coordinate patch, and which are not?

(c) Calculate and construct an embedding diagram for the spacelike hypersurface $t = 0$, $0 < \bar{r} < \infty$.

(d) Find a coordinate transformation that interchanges the region near $\bar{r} = 0$ with the region near $\bar{r} = \infty$, while leaving the metric coefficients in their original form.

Exercise 31.8. REISSNER-NORDSTRØM GEOMETRY

(a) Solve the Einstein field equations for a spherically symmetric, static gravitational field

$$ds^2 = -e^{2\Phi(r)}\, dt^2 + e^{2\Lambda(r)}\, dr^2 + r^2(d\theta^2 + \sin^2\theta\, d\phi^2),$$

with no matter present, but with a radial electric field $\boldsymbol{B} = 0$, $\boldsymbol{E} = f(r)\boldsymbol{e}_{\hat{r}}$ in the static orthonormal frame

$$\boldsymbol{\omega}^{\hat{t}} = e^{\Phi}\,\boldsymbol{dt}, \qquad \boldsymbol{\omega}^{\hat{r}} = e^{\Lambda}\,\boldsymbol{dr}, \qquad \boldsymbol{\omega}^{\hat{\theta}} = r\,\boldsymbol{d\theta}, \qquad \boldsymbol{\omega}^{\hat{\phi}} = r\sin\theta\,\boldsymbol{d\phi}.$$

Use as a source in the Einstein field equations the stress-energy of the electric field. [*Answer:*

$$\boldsymbol{E} = (Q/r^2)\boldsymbol{e}_{\hat{r}}, \tag{31.24a}$$

$$ds^2 = -\left(1 - \frac{2M}{r} + \frac{Q^2}{r^2}\right)dt^2 + \left(1 - \frac{2M}{r} + \frac{Q^2}{r^2}\right)^{-1} dr^2 + r^2(d\theta^2 + \sin^2\theta\, d\phi^2). \tag{31.24b}$$

This is called the "Reissner (1916)-Nordstrøm (1918) metric".]

(b) Show that the constant Q is the total charge as measured by a distant observer ($r \gg 2M$ and $r \gg Q$), who uses a Gaussian flux integral, or who studies the coulomb-force-dominated orbits of test charges with charge-to-mass ratio $e/\mu \gg M/Q$. What is the charge-to-mass ratio, in dimensionless units, for an electron? Show that the constant M is the total mass as measured by a distant observer using the Keplerian orbits of electrically neutral particles.

(c) Show that for $Q > M$, the Reissner-Nordstrøm coordinate system is well-behaved from $r = \infty$ down to $r = 0$, where there is a physical singularity and infinite tidal forces.

(d) Explore the nature of the spacetime geometry for $Q < M$, using all the techniques of this chapter (coordinate transformations, Kruskal-like coordinates, studies of particle orbits, embedding diagrams, etc.).

[*Solution:* see Graves and Brill (1960); also Fig. 34.4 of this book.]

(e) Similarly explore the spacetime geometry for $Q = M$. [*Solution:* see Carter (1966b).]

(f) For the case of a large ratio of charge to mass [$Q > M$ as in part (c)], show that the region near $r = 0$ is unphysical. More precisely, show that any spherically symmetric distribution of charged stressed matter that gives rise to the fields (31.24) outside its boundary must modify these fields for $r < r_0 = Q^2/2M$. [Hint: Study the quantity $m(r)$ defined in equations (23.18) and (32.22h), noting its values deduced from equation (31.24), on the one hand, and from the appropriate Einstein equation within the matter distribution, on the other hand. See Figure 26 of Misner (1969a) for a similar argument.]